

CITY UNIVERSITY OF HONG KONG
DEPARTMENT OF
PHYSICS AND MATERIALS SCIENCE

BACHELOR OF ENGINEERING (HONS) IN MATERIALS ENGINEERING

2010-2011

DISSERTATION

Porous Gradient Materials for Analysis Applications

by

TANG CHUN TING

March 2011

Porous Gradient Materials for Analysis Applications

By

TANG CHUN TING

Submitted in partial fulfilment of the
requirements for the degree of
BACHELOR OF ENGINEERING (HONS)
IN
MATERIALS ENGINEERING
from
City University of Hong Kong

March 2011

Project Supervisor :

Yangyang Li

Table of Contents

Acknowledgements	-----	(iii)
List of Figures	-----	(iv-vi)
List of Tables	-----	(vi)
Abstract.	-----	(vii)
Objective	-----	(1)
1. Introduction	-----	(1-2)
2. Literature review	-----	(3-13)
2.1 Nanotechnology	-----	(3)
2.2 Synthesis methods for nanostructure oxides	-----	(3)
2.2.1 Thermal evaporation method	-----	(3-4)
2.2.2 Gas reaction method	-----	(4)
2.2.3 Template method	-----	(4-5)
2.2.4 Solution-phase process method	-----	(5)
2.3 Anodizing	-----	(5-8)
2.4 Cold rolling	-----	(8-9)
2.5 Graded Porosity Silicon Films Fabrication	-----	(9-10)
2.6 Gradient TiO ₂ nanotube arrays	-----	(10-13)
2.6.1 Fabrication for Gradient TiO ₂ nanotube arrays	-----	(11)
2.6.2 Feature of Gradient TiO ₂ nanotube arrays	-----	(11-12)
2.6.3 Application for gradient TiO ₂ nanotube arrays	-----	(13)

3. Methodology	-----	(14-17)
3.1 Preparation of Ti foil	-----	(14)
3.2 Preparation of Electrolyte Solution	-----	(14)
3.3 Setting up the equipment	-----	(14-15)
3.4 Anodization	-----	(16)
3.5 Analysis by SEM	-----	(16-17)
4. Result and Discussion	-----	(18-33)
4.1 Data of Results	-----	(18-24)
4.2 Comparing the nanostructure of rolled samples and without rolled samples	-----	(24-25)
4.3 Comparing the nanostructure between the different values of % cold work	-----	(26-27)
4.4 Comparing the nanostructure between the different times for anodization	-----	(27-29)
4.5 Comparing the nanostructure between the different voltages for Anodization	-----	(29-30)
4.6 Reason for the rolling effects of the nanostructure	-----	(31)
4.7 Different morphologies of the nanostructure	-----	(31-33)
5. Conclusion	-----	(34)
6. Reference	-----	(35-38)

Acknowledgements

I would like to express my sincerest gratitude to my supervisor, second assessor and my FYP lab tutor. Firstly, I would like to thank my supervisor, Dr. YangYang Li. She is a good teacher who patiently gives me guidance and support. She is always available for me to ask she question and assist me solve the problem. Secondly, I would like to thank my second assessor, Professor Robert Li. He has forwardly reminded me some knowledge I have missed or not enough. I feel very helpful for his reminding about missed knowledge and work on schedule. Li Hui is my FYP lab tutor who is very enthusiastic. Her guidance is very important and helpful. She always supports me and assists me during the lab. Many techniques in the lab are taught by her. I would like to heartfelt thanks to her help. Finally, I would like to thank Fengxia and Jessie. They teach me how to do the FYP lab and give me a lot of techniques support.

List of Figures

Figure No.	Title	Page.
Fig.2.3a	Depiction of an electrochemical cell in which the Ti samples are anodized.	5
Fig.2.3b	Cross section of anodizing process.	6
Fig.2.3c	The color spectrum for specific voltage levels.	7
Fig.2.3d	Specific thickness of the oxide layer; therefore, constructive interference occurs.	8
Fig.2.4a	A transmission electron micrograph of titanium alloy in which the dark lines are dislocations.	8
Fig.2.5a	Photographs of graded porosity Si films prepared using the electrochemical cell and electrode arrangement from Figure 1. Values of HF(aq)/EtOH are: 1:1 (A), 2:1 (B), and 3:1 (C).	10
Fig.2.6a	Schematic diagram of the anodization setup used to fabricate the gradient TiO ₂ nanotube arrays.	11
Fig.2.6.2a	SEM top and side images of a TiO ₂ nanotube.	12
Fig.2.6.3a	The optical photographs and reflectivity spectra of a gradient TiO ₂ film in air (a), ethanol vapor (b), and hexane vapor (c). The film was fabricated via anodization at 100 V for 5 min.	13

Fig.3.3a	Schematic diagram of the anodization setup used to fabricate the TiO ₂ nanotube arrays.	14
Fig.3.3b	Set up the equipment.	15
Fig 3.4a	A Ti foil before anodization (left) and after anodization (right).	16
Fig.4.1a	The optical photographs of a gradient TiO ₂ film.	18
Fig. 4.1b	Top-view SEM images of a gradient TiO ₂ film (Sample A) at x = 0, 2, 4, 6, 8, 10 mm (a-f, respectively). The film was fabricated by a Ti foil of 60% cold work and anodization at 100 V for 20 min.	20
Fig. 4.1c	Side-view SEM images of the gradient TiO ₂ film (Sample A) at x = 0, 2, 4, 6, 8, 10 mm (a-f, respectively). The film was fabricated by a Ti foil of 60% cold work and anodization at 100 V for 20 min.	21
Fig.4.1d	The distribution for the hole size of the TiO ₂ nanotubes on the sample plane.	23
Fig.4.1e	The distribution for the length of the TiO ₂ nanotubes on the sample plane.	24
Fig.4.2a	Hole size distribution of samples A, G.	24
Fig.4.2b	Nanotube length distribution of samples A, G.	25

Fig.4.3a	Hole size distribution of samples C, E, F.	26
Fig.4.3b	Nanotube length distribution of samples C, E, F.	26
Fig.4.4a	Hole size distribution of samples A, B.	27
Fig.4.4b	Nanotube length distribution of samples A, B.	28
Fig.4.5a	Hole size distribution of samples A, C.	29
Fig.4.5b	Nanotube length distribution of samples A, C.	30
Fig.4.7a	Different morphologies (a. porous, b. tubular) are obtained by electrochemical anodization of metallic titanium.	31
Fig. 4.7b	Top-view SEM images of a gradient TiO ₂ film of Sample A to F at x = 0 (no. A-F respectively).	32

List of Tables

Table4.1a	The different conditions of samples for anodization	19
Table4.1b	The hole size of nanotube for different distance	22
Table4.1c	The tube length of nanotube for different distance	13

Abstract

Gradient TiO₂ nanotube arrays were synthesized by anodization with an asymmetric electrode configuration. A gradually changing distribution of tube diameters and length were appeared across the sample surface. Such material has proven an interesting matrix for sensing and screening applications.

In order to study the growth control of nanostructure, cold rolling and following anodization with asymmetric electrode configuration were performed to fabricate gradient TiO₂ nanotube arrays.

The tube diameters and length of nanotube arrays were decreased due to cold rolling. By adjusting the anodization time and voltage, different result of tube diameters and length for rolled sample could be observed. The tube diameters and length of nanotube arrays were studied by SEM. The decreasing tube diameters and length are dependent on the % cold work. When the % cold work is high, the decreasing tube diameters and length will be high.

Objective

Porous gradient materials have proven an interesting matrix for sensing and screening applications. However, the fabricating difficulties remain an obstacle in this field. In this project, the objectives include the following points.

1. Fabricate Gradient TiO₂ nanotube arrays.
2. Study the effect of cold rolling for the TiO₂ nanostructure.
3. Analyse the effect of different anodization condition for the rolled Ti foil.
4. Study a method to control the growth of TiO₂ nanostructure.

1 Introduction

Close attention has been drawn to nanoscale material because of their unique properties and application. Their structural features, such as high surface to volume ratios and size dependent properties are very important features. In recent years, ordered TiO₂ nanotube arrays have been studied and their outstanding charge transport properties were indicated. Highly ordered TiO₂ nanotube arrays have demonstrated many applications in photocatalysts, dye-sensitized solar cells, electro-chromic films, biomedicine, photovoltaics, superhydrophobic and superhydrophilic materials. TiO₂ is the most studied material because of its broad range of functional properties. Different synthesis strategies of nanotubular TiO₂ film structures have been reported in recent years. These synthesis strategies include template based methods, hydrothermal processes, sol-gel transcription using organo-gelators as templates, electroless deposition methods and anodic oxidation of

titanium. Within these methods, anodization is the most prominent one because their dimensions can be precisely controlled [1-6, 30-32].

During the anodization, many parameters can be changed to control the diameter and length of the anodic TiO₂ nanotubes. These parameters include anodization voltage or current, the anodization time and the electrolyte composition. Various morphologies of the nanomaterial can be fabricated by changing the anodization voltage or the electrolyte composition. In this project, a gradient TiO₂ nanotube array was studied to change their diameter and length by cold rolling [1, 2, 5].

In gradient TiO₂ nanotube arrays, their nanotube diameter and length are gradually changing across the sample plane. Anodization using an asymmetric electrode configuration is a method to fabricate gradient TiO₂ nanotube arrays. Other porous gradient structures such as “porous silicon films with a distribution of pore size” also can be constructed by an asymmetrically applied electric field electrochemical method. The potential applications of porous gradient structures include size-selective biosensors and screening devices for chemical and biology assays [5, 30].

From the paper “Gradient TiO₂ nanotube arrays [5]”, the hole diameter of fabricated TiO₂ nanotubes gradually change from 110 to 42 nm and the length of TiO₂ nanotubes decrease from 14 μm to 2 μm. In this project, the effect of cold rolling before anodization was studied to change the hole diameter and tube length of TiO₂ nanotubes. Cold rolling is a method of work hardening that can be used to increase the strength of metal. After cold rolling before anodization, the hole diameter and tube length of TiO₂ nanotubes will decrease. The effect of different anodization time and voltage in rolled sample will also be studied in this project [1-5, 24].

2 Literature review

2.1 Nanotechnology

“Nano” is a unit of size in 10^{-9} m, which is bigger than atoms but can't be saw by using light microscope. To deal with this small size of material is called Nanotechnology. 1D nanomaterials can be classified by different materials which include carbon, silicon, III-V compound semiconductor, II-VI compound semiconductor and Oxides. Morphologies of 1D nanomaterials include nanotubes, nanowires, nanorods, nanocables, nanoribbons, nanosheet, etc... Four synthesis mechanisms of nanomaterials are Metal-catalyzed “VLS (Vapor-Liquid-Solid)” mechanism, “OAG (Oxide-Assisted Growth)” mechanism, “VS (Vapor-Solid)” mechanism and “SLS (Solution-Liquid-Solution)” mechanism [20].

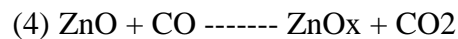
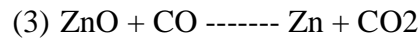
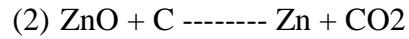
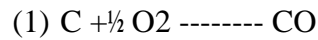
2.2 Synthesis methods for nanostructure oxides

Nanostructure oxides including MgO, ZnO, CaO, SnO, SnO₂, PbO₂, TiO₂, SiO₂, MnO₂, In₂O₃, Ga₃O₃, Cu₂O, WO₃... Nanostructure oxides can be synthesis by thermal evaporation method, gas reaction method, template method and solution-phase process method [20].

2.2.1 Thermal evaporation method

In Thermal evaporation method, source materials are vaporized at high temperature and the vapor are condensed under certain temperature, pressure, atmosphere and substrate to form the desired products. Tube furnace is used to conduct this process [20].

At high temperature (1373 K), Zn or Zn suboxides are reduced by carbon via the following reactions [20]:

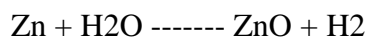


At low-temperature site (lower than 1180 K), Zn vapor are produced and condensed on the inner wall of the quartz tube forming liquid droplets. These are ideal nuclei of ZnO nanowires via the VLS mechanism [20].

2.2.2 Gas reaction method

In this method, source material powder is heated in the horizontal tube furnace directly. Oxide nanorods with 10-200nm diameters are fabricated by a simple gas reaction method. All of the nanorods are hexagonal and about several to tens of microns length [20].

The reaction equation for synthesis zinc oxide nanorods is :



Through the oxide-assisted growth, zinc oxide nanorods are synthesized [20].

2.2.3 Template method

Template methods include wet method and dry method. A channel of anodic aluminium oxide is used as a template. In wet method, electrophoretic deposition is utilized to grow the source material nanowires into the channels. In dry method, physical phase evaporation and condensation are utilized to grow the source material

nanowires inside the channels [20].

In a tube furnace, nanowire was growth and about 10nm gold layer was sputtered on anodic aluminium oxide (AAO) template as catalyst. The Zn source and AAO template were heated in an alumina boat [20].

2.2.4 Solution-phase process method

Reduction and following by oxidation of ZnS powders at 1300° C are used to synthesis the large-quantity growth of hexagonal prismatic ZnO whiskers. The whiskers are structurally uniform with about 350nm diameter and up to 15µm length, and are single crystalline in nature. They grow along the [001] crystallographic direction and have hexagonal cross sections [20].

2.3 Anodizing

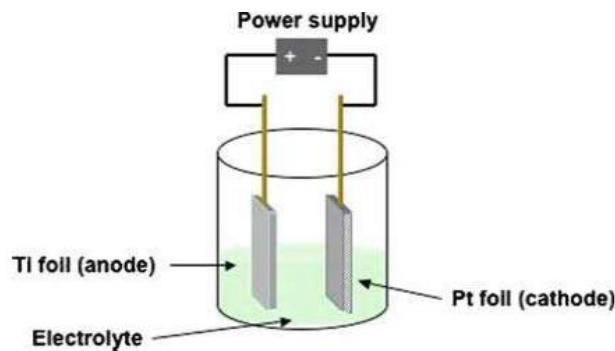


Fig.2.3a Depiction of an electrochemical cell in which the Ti samples are anodized [22].

Anodizing is an electrochemical process used to increase the thickness of the oxide layer on the surface of metal. The thickness and properties of this layer are dependent on the metal. Aluminium and tantalum are the most commonly used. The oxide layer will be formed at the anode electrode of an electrical circuit, so the process is called

“Anodizing” [8-9].

In order to remove the oils and greases, metal should be cleared by weak alkaline solutions. The surface is etched to remove heavy oxides. Rinsing is needed to clean the metal [8-9].

A metal is immersed in acidic electrolytes. First, the anode is set up by connecting it to the positive terminal of a dc power supply. Cathode is connected to negative terminal of the power supply. Cathode can be any electronic conductor that is unreactive (inert) in the anodizing bath. A DC (direct current) electric current is flow through the anode (metal be anodise) and cathode to start the anodizing. [8-9]

When the current flows through the circuit, the water in the electrolyte will break down and oxygen will deposited at the anode. Reactions will occur between the oxygen and metal at the anode to form the oxide. The oxide film is built and present on the surface of anode as shown in Fig.2.3b [8-9].

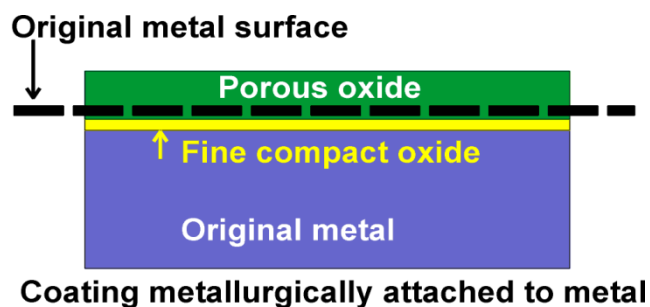


Fig.2.3b Cross section of anodizing process [8].

On the other hand, the oxide film will be dissolved by the acid in the electrolyte and the porous oxide film will be formed on the metal surface. After the required thickness of anodic film is formed, the metal is removed from the electrolyte and rinsing is needed to remove the acids from the surface of the film [8-10].

During the anodizing process, the thickness of the oxide layer will increase as the voltage increases. Certain colors will appear at specific voltage levels due to the optical properties and thickness of the oxide coating. The colors are gradually changed through a limited spectrum as shown in Fig.2.3c [8, 11].

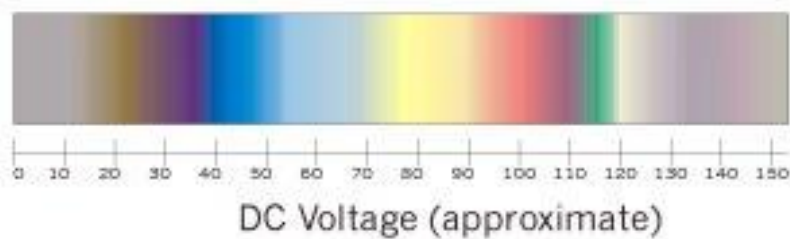


Fig.2.3c The color spectrum for specific voltage levels [11].

The color apparent in the metal is caused by interference between certain wavelengths of light reflecting off the metal and oxide coated surface. When the light comes to the surface of oxide layer, a part of light will reflect from the surface, other light will pass through the oxide surface and be reflected on the metal surface. Light passing through the oxide layer and reflecting from the metal will travel farther than the light reflecting from the oxide layer [11].

When there is specific thickness of the oxide layer, one wave pattern is closely synchronized with other. Then the wave strength will be increased (constructive interference) and particular color will appear brighter [11].

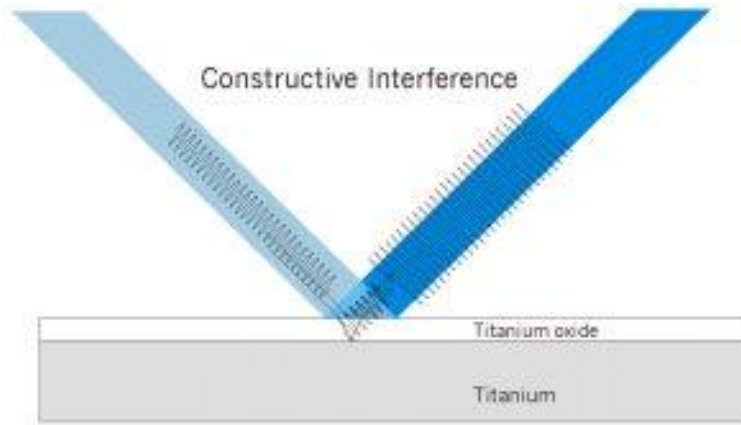


Fig.2.3d Specific thickness of the oxide layer; therefore, constructive interference occurs [11].

2.4 Cold rolling

Cold working, also call as strain hardening or work hardening, is the strengthening of a metal through plastic deformation. After the cold rolling, dislocation will move within the crystal structure of material and cause the strengthening [17-19, 21].



Fig.2.4a A transmission electron micrograph of titanium alloy in which the dark lines are dislocations [19].

Percent cold work (% CW) is used to express the degree of plastic deformation [19]:

$$\%CW = \frac{A_o - A_d}{A_o} \times 100$$

Where A_0 = original cross sectional area

A_d = cross sectional area after deformation

After the cold rolling, yield strength and hardness are increasing but ductility is decreasing. [17-19, 21,24]

2.5 Graded Porosity Silicon Films Fabrication

In order to prepare the Porous Si films containing a distribution of pore sizes, electrochemically etching silicon with asymmetric electrode configuration would be used. The distance from the Pt counter electrode will affect the potential at the Si electrode solution interface because of the solution resistance. The current density will decrease when the distance from the counter electrode increases. The pores ranging in size from 2-1500 nm can be generated in highly boron-doped silicon substrates by changing the current density. The pore size also can be affected by the ratio of aqueous HF/ethanol [1-4, 29-32].

A current density gradient across the wafer will be provided due to asymmetric electrode configuration. Therefore the morphology of the pores will have distinct change as shown in Figure 2.5a [1-4].

Four distinct regions are appeared on the etched area of the Si wafer. The region has a shiny appearance and contains no porous structure that is closest to the Pt counter electrode with the highest current density. The porous Si can only be generated below a critical current density value. The Si would dissolve uniformly when above the critical value. It will lead to the smooth electropolished material observed. Fig. 2.5aA1 shows a region next to the electropolished area. It is a transitional region consisting of an incompletely electropolished surface film of porous Si with small

features. Fig. 2.5aA2 shows a small area next to the transitional region. It appears matted to the eyes. In this region, there is a high porosity Si, which is susceptible to cracking and peeling upon drying. Fig. 2.5aA3 shows a region adjacent to reflective porous Si. The porous Si gradient films display a rainbow light because of the continuously changing lateral rejection band distribution [1-4].

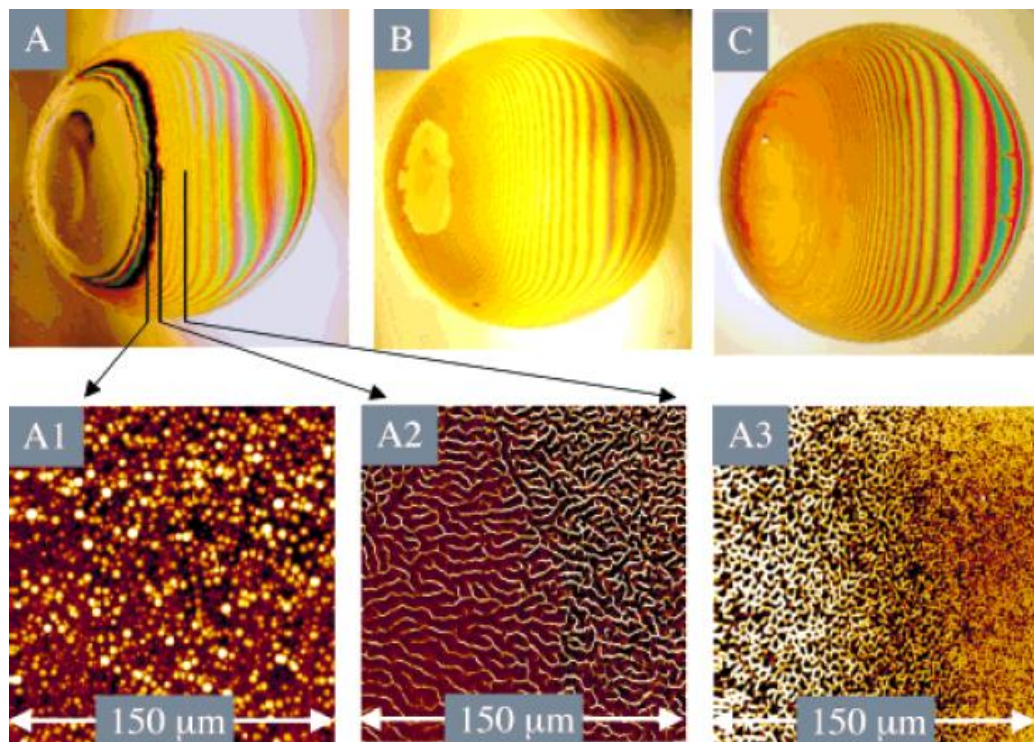


Fig.2.5a Photographs of graded porosity Si films prepared using the electrochemical cell and electrode arrangement from Figure 1. Values of HF(aq)/EtOH are: 1:1 (A), 2:1 (B), and 3:1 (C) [1].

2.6 Gradient TiO₂ nanotube arrays

Gradient TiO₂ nanotubes arrays can be fabricated by anodic oxidation of titanium foil with asymmetric two electrode configuration [5-6].

2.6.1 Fabrication for Gradient TiO₂ nanotube arrays

In order to fabricate the gradient TiO_2 nanotubes arrays, the titanium foil should be pressed with an Al foil against an O-ring in electrochemical cell. The electrolyte was prepared by an ethylene glycol solution containing Hydrogen fluoride and Hydrogen peroxide. The electrolyte should be aged before carrying out the anodization. The anodization would be start by using a constant voltage for a period of time. After the above process, gradient TiO_2 films can be produced [5-6, 29-32].

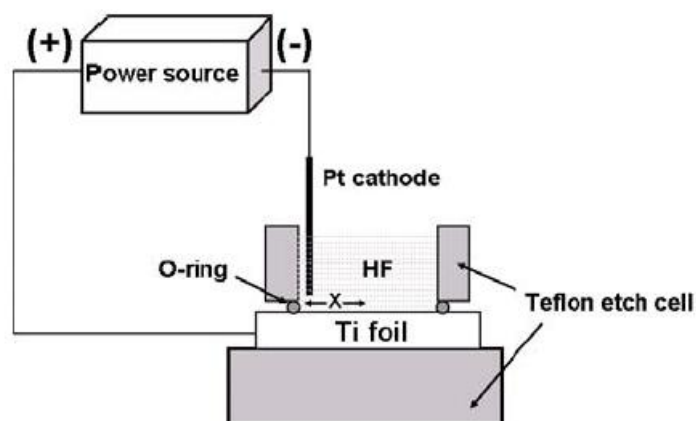


Fig.2.6a Schematic diagram of the anodization setup used to fabricate the gradient TiO_2 nanotube arrays [5].

2.6.2 Feature of Gradient TiO_2 nanotube arrays

The outer and inner diameter of gradient TiO_2 nanotubes can be changed by adjusting the distance (value x) from the point on the sample closest to the Pt cathode to the position of interest on the sample. The outer and inner diameter of gradient TiO_2 nanotubes will decrease, when the value x increases or leaves the Pt cathode. The gradient TiO_2 nanotubes length would also be decreased. The above change is due to the IR – drop in the electrolyte. When a current is passed between the counter electrode and working electrode, there is voltage drop in both electrodes. The

potential measurement of ideal location should be inside the double layer at the working electrode. Part of the voltage drop between a counter electrode (CE) and a working electrode (WE) would be added to the WE potential. This error is called IR – drop. On the other hand, the apply anodization voltage is the main factor for the change in the inner and outer tube diameters and film thickness [5-6, 8, 29-32].

After the anodization of the gradient TiO_2 film, the film will display a rainbow-like appearance. It is because the optical thickness changes gradually across the TiO_2 surface. The optical features of the gradient TiO_2 film will changes, when exposed to ethanol and hexane vapors. Therefore the gradient TiO_2 film could be used for optical sensing. The optical features of the gradient TiO_2 film at a certain position is determined by the film optical thickness at that specific position. If the pores of the gradient TiO_2 film are filled with other species, the increasing thickness of the film would cause the observed shift of the optical features of the film. It is because of the pore size and the film thickness that can be gradually changed across the sample plane. Ggradient TiO_2 nanotube arrays can be used as vapor sensors, size-elective biosensors and screening devices for chemical and biology assays [5-6, 29-30].

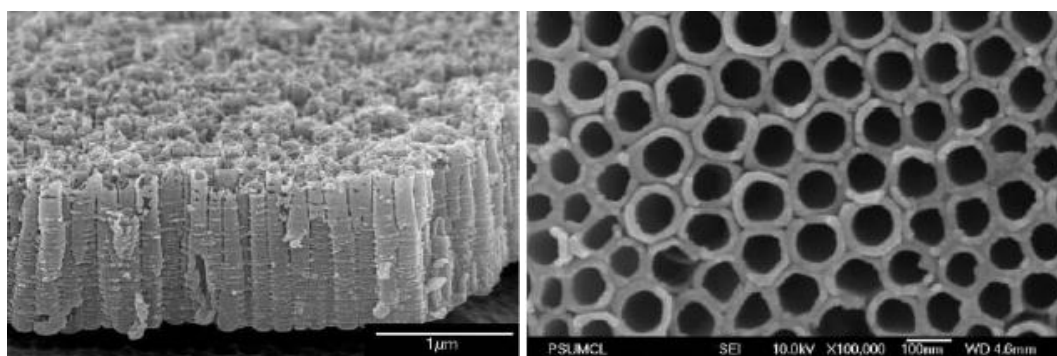


Fig.2.6.2a SEM top and side images of a TiO_2 nanotube [6]

2.6.3 Application for gradient TiO₂ nanotube arrays

An observation study has reported about the potential application of gradient TiO₂ films for optical sensing. The optical features of the gradient TiO₂ film can be changed upon exposure to ethanol and hexane vapours. The optical response of the gradient TiO₂ film is determined by the film optical thickness at that specific position. For the optical sensing, gradient TiO₂ film is filled with other species such as ethanol or hexane vapours. The shift of the optical features of the film is observed due to the optical thickness of the film increases [5].

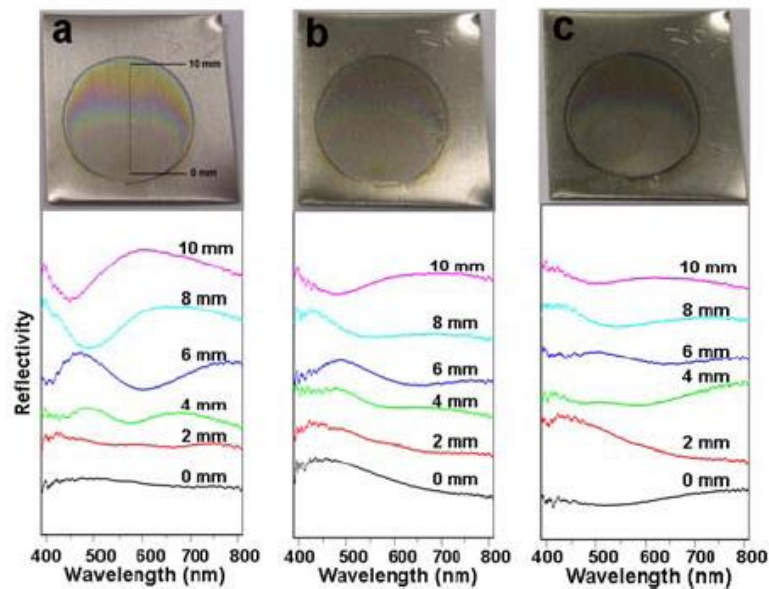


Fig.2.6.3a The optical photographs and reflectivity spectra of a gradient TiO₂ film in air (a), ethanol vapor (b), and hexane vapor (c). The film was fabricated via anodization at 100 V for 5 min [5].

3 Methodology

3.1 Preparation of Ti foil

A Ti foil was rolled by cold roll machine for different % cold work. The different % cold work for the Ti foil are 32%, 52% and 60% respectively.

A Ti foil was cut into a number of 1.8 x 1.8cm squares. The square Ti foil (0.25mm thick) was washed by acetone, water, and ethanol respectively for 30min each. After washing, Ti foil was purged with pure Nitrogen.

3.2 Preparation of Electrolyte Solution

0.738ml HF and 1.1ml H₂O₂ were added to 100ml ethylene glycol solution as electrolyte. The solution was aged for 12 hours at 60V.

3.3 Setting up the equipment

The equipment was set up for anodic oxidation of a Ti foil using an asymmetric two-electrode configuration as shown in Fig.4.

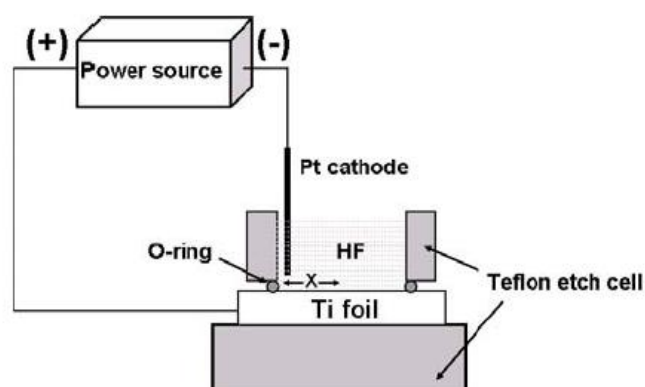


Fig.3.3a Schematic diagram of the anodization setup used to fabricate the TiO₂ nanotube arrays.

The Ti foil was pressed together with an Al foil against an O-ring (1.1cm) in the electrochemical cell. The Pt wire was used as cathode and placed 1mm higher than the surface of the Ti anode. The distance between Pt cathode and the inner edge of O-ring should be 1mm. The fume chamber should be closed and the HF electrolyte was dropped to the etched cell. Pt cathode and Al foil should be connected to a Sourcemeter which was connected to a computer.

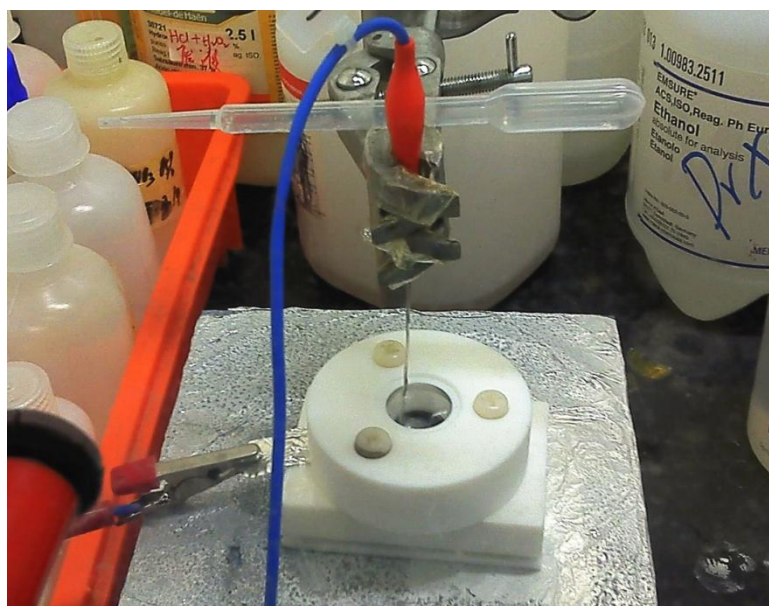


Fig.3.3b Set up the equipment.

3.4 Anodization

Anodization was carried out by using a constant voltage for a period of time. The samples were produced by repeating the anodization process. The voltage and time for anodization should be (A) 100V 20min for 60% cold work, (B) 100V 10min for 60% cold work, (C) 60V 20min for 60% cold work, (D) 100V 20min for 52% cold work, (E) 60V 20min for 52% cold work, (F) 60V 20min for 32% cold work respectively.

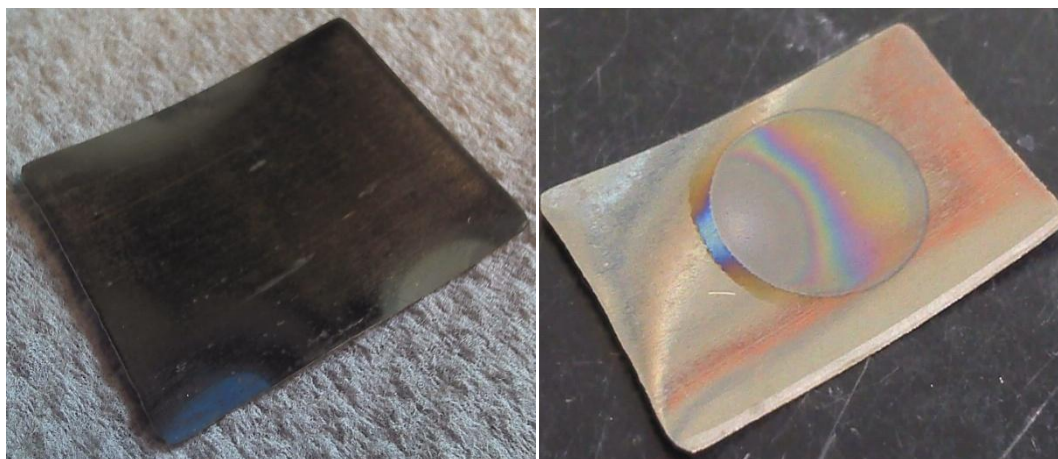


Fig 3.4a A Ti foil before anodization (left) and after anodization (right).

3.5 Analysis by SEM

Scanning electron microscopy (SEM) was used to analyse the sample. Multiple points on the oxide surface were chosen to analyse each sample in order to get the hole size of nanotubes. First, a point was chosen on the oxide surface, which was the closest to anodization cathode. Next, a 2mm gap was allowed between the first point and the second point, following the centre line of the gradient direction. A 2mm gap was allowed between the second point and the third point, following the same direction. The same method was used to analyse the sample right up to 10mm from the first point or no nanostructure was found.

After all the oxides surfaces were analysed by SEM, the centre line of gradient direction was followed to cut the sample into 2 pieces. One piece of that sample was chosed for analysis by SEM in order to get the length of the nanotubes. First, a point was chosen on the oxide surface, which was the closest to anodization cathode. Next, a 2mm gap was allowed between the first point and the second point, following the centre line of the gradient direction. A 2mm gap was allowed between the second point and the third point, following the same direction. The same method was used to analyse the sample right up to 10mm from the first point or no nanostructure was find.

4 Results and Discussion

4.1 Data of Results

By using the anodization with asymmetric distributed electric field, a gradient TiO₂ nanotube arrays can be fabricated. The tube diameters and length across the sample plane gradually changed and a rainbow colour could be observed in the sample surface (Fig.4.1a).

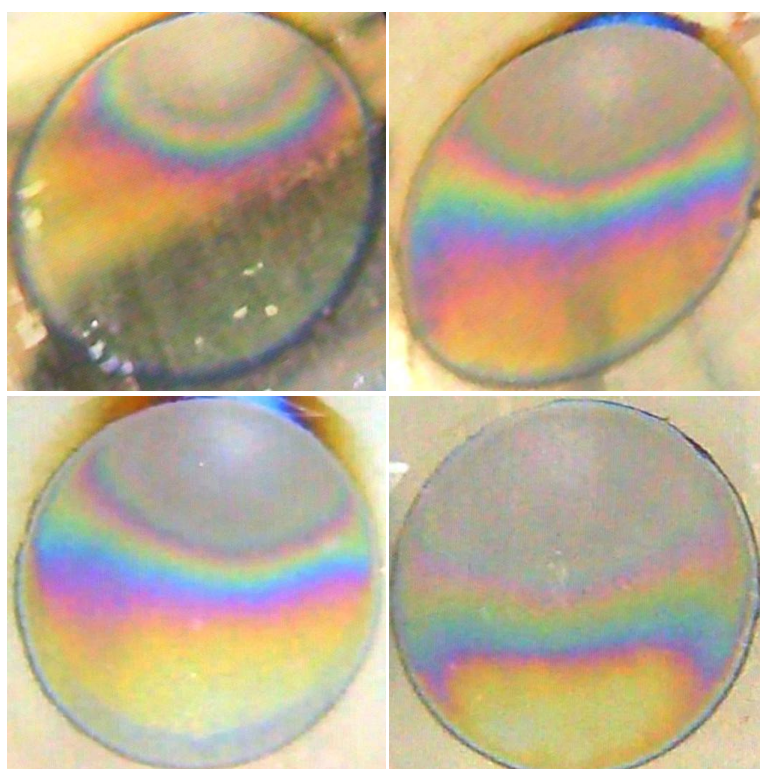


Fig.4.1a The optical photographs of a gradient TiO₂ film.

In the experiment, rolled Ti foils were used to fabricate the gradient TiO₂ nanotube arrays. After cold rolling and anodization, the TiO₂ nanotube was studied to find out the changes by using SEM. Different rolling conditions of Ti foils are used and the sample data are shown in Table4.1a.

Table4.1a The different conditions of samples for anodization

	% Cold Work	Anodization Voltage	Anodization Time
Sample A	60%	100V	20min
Sample B	60%	100V	10min
Sample C	60%	60V	20min
Sample D	52%	100V	20min
Sample E	52%	60V	20min
Sample F	32%	60V	20min
Sample G	0%	100V	20min

Cold working is a way to increase the strength of metal (strengthening) and cold rolling is a method of cold working. % cold work is a value to explain the percentage changing of the sample. The effects of different % cold working for nanotube will be discussed in the following paragraph.

Through the SEM, the nanostructure, such as hole size and tube length, can be studied and the data are shown in Table4.1b and Table4.1c.

Without rolled sample anodization at 100 V for 20 min was studied by recent report [5] and called sample G in this report. The nanostructure data of sample G in Table4.1b and Table4.1c is derived from that report [5].

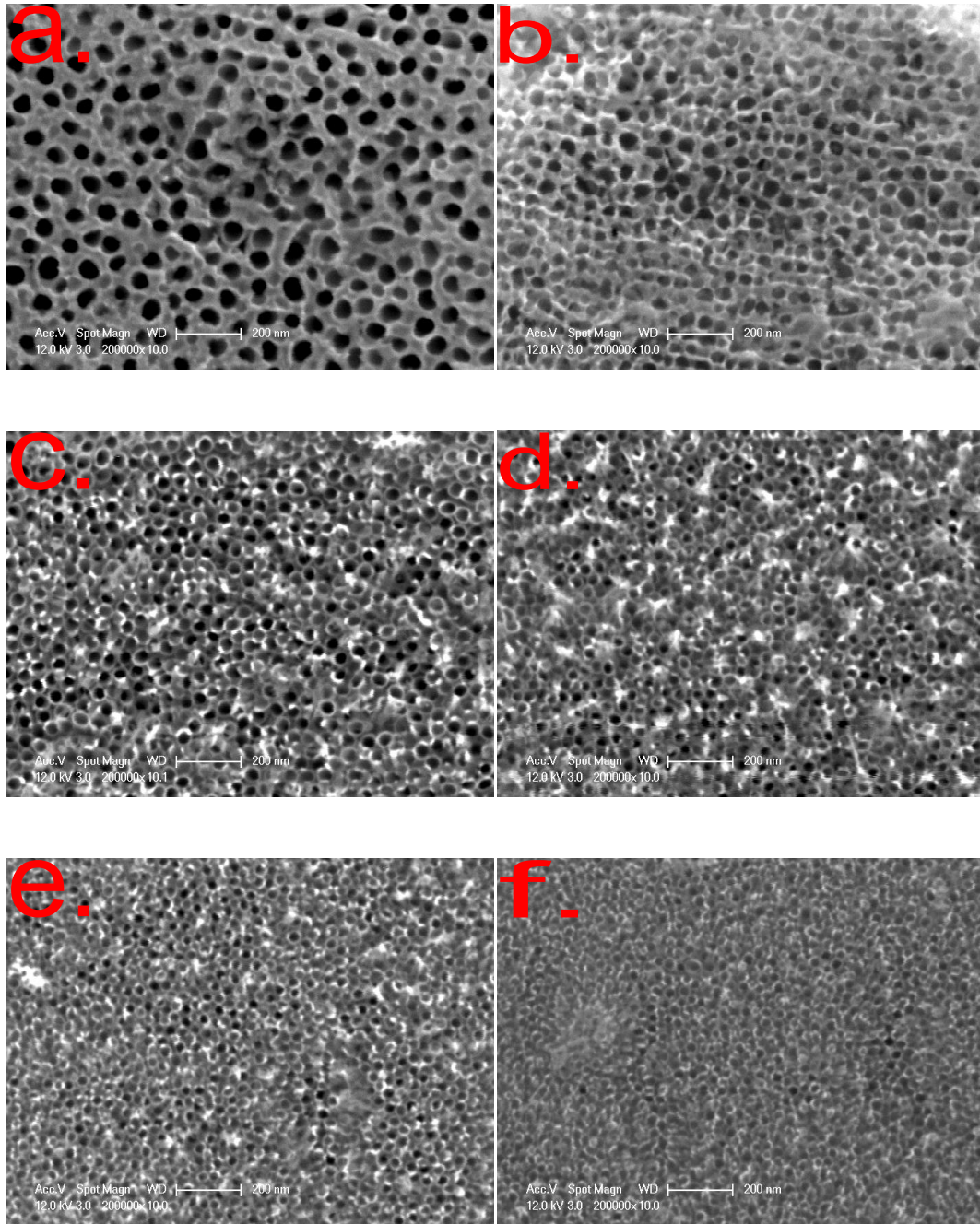


Fig. 4.1b Top-view SEM images of a gradient TiO₂ film (Sample A) at $x = 0, 2, 4, 6, 8, 10$ mm (a-f, respectively). The film was fabricated by a Ti foil of 60% cold work and anodization at 100 V for 20 min.

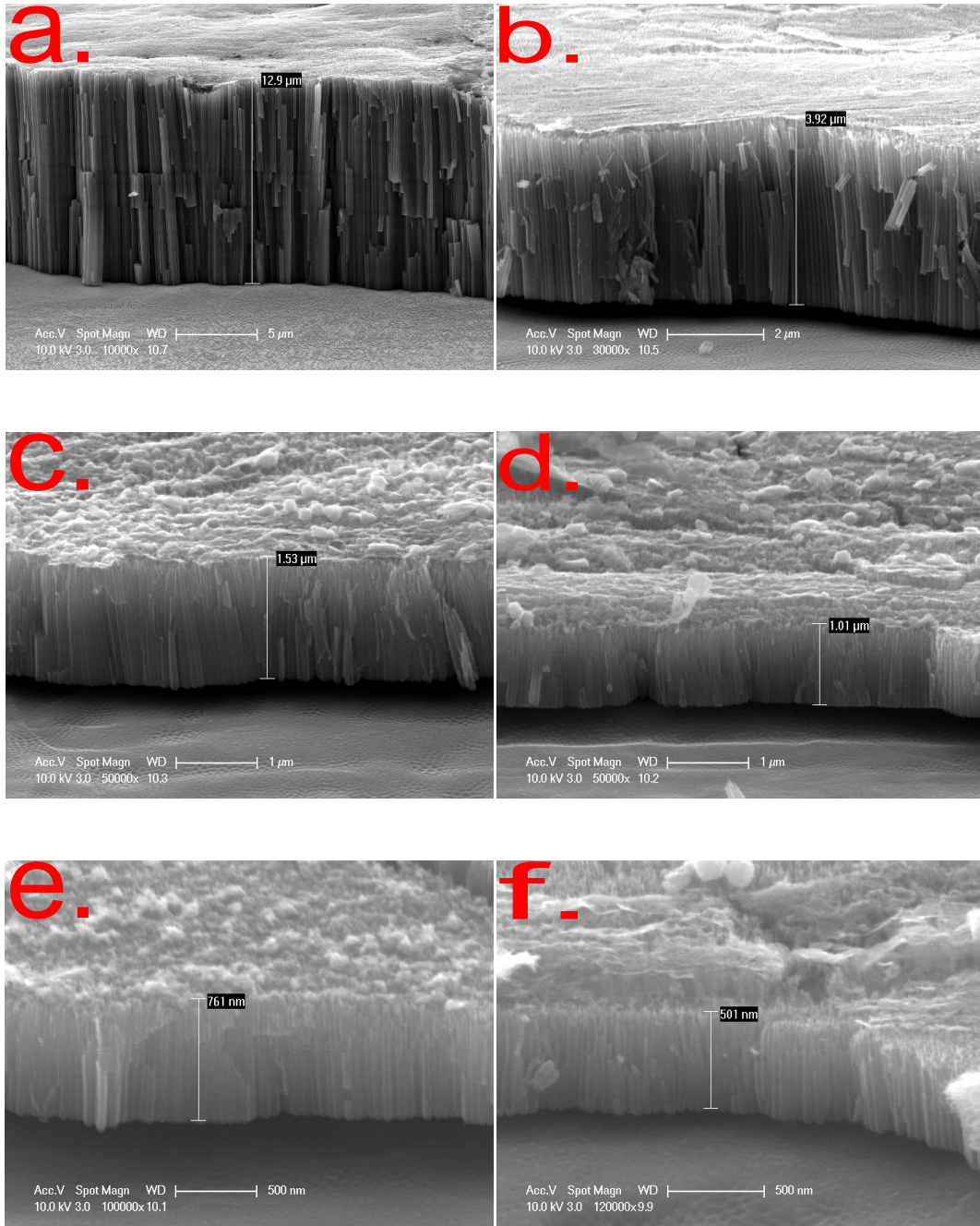


Fig. 4.1c Side-view SEM images of the gradient TiO₂ film (Sample A) at $x = 0, 2, 4, 6, 8, 10$ mm (a-f, respectively). The film was fabricated by a Ti foil of 60% cold work and anodization at 100 V for 20 min.

Table4.1b The hole size of nanotube for different distance

	x = 0mm	x = 2mm	x = 4mm	x = 6mm	x = 8mm	x = 10mm
Sample A	67.4nm	46.9nm	35.9nm	26.4nm	21.2nm	18.3nm
Sample B	28.6nm	20.5nm	13.2nm	9.5nm		
Sample C	37.1nm	27.8nm	20.5nm			
Sample D	92.2nm	46.2nm	32.2nm	22.0nm	18.3nm	15.4nm
Sample E	38.1nm	29.3nm	16.1nm			
Sample F	59.6nm	30.7nm	22.7nm			
Sample G	110nm	80nm	60nm	60nm	50nm	42nm

The value of x is the distance between an observing point on sample surface and the point on the sample that is the closest to the Pt cathode. When the x is high, its observing point is far from the cathode during anodization.

When the value of x is increased, the diameter of the TiO₂ nanotubes will gradually decrease. The gradually decreasing of the nanotube diameters and length across the sample plane was caused by the IR drop in the electrolyte [5].

Table4.1c The tube length of nanotube for different distance

	x = 0mm	x = 2mm	x = 4mm	x = 6mm	x = 8mm	x = 10mm
Sample A	12.60 μm	6.32 μm	1.53 μm	1.01 μm	0.63 μm	0.50 μm
Sample B	3.19 μm	3.13 μm	1.02 μm	0.51 μm	0.30 μm	0.22 μm
Sample C	1.19 μm	2.66 μm	1.21 μm			
Sample D	6.93 μm	3.04 μm	1.44 μm	1.04 μm	0.81 μm	0.66 μm
Sample E	2.50 μm	1.07 μm				
Sample F	3.11 μm	1.29 μm	0.69 μm	0.29 μm		
Sample G	14.00 μm	6.60 μm	3.60 μm	2.70 μm	2.30 μm	2.00 μm

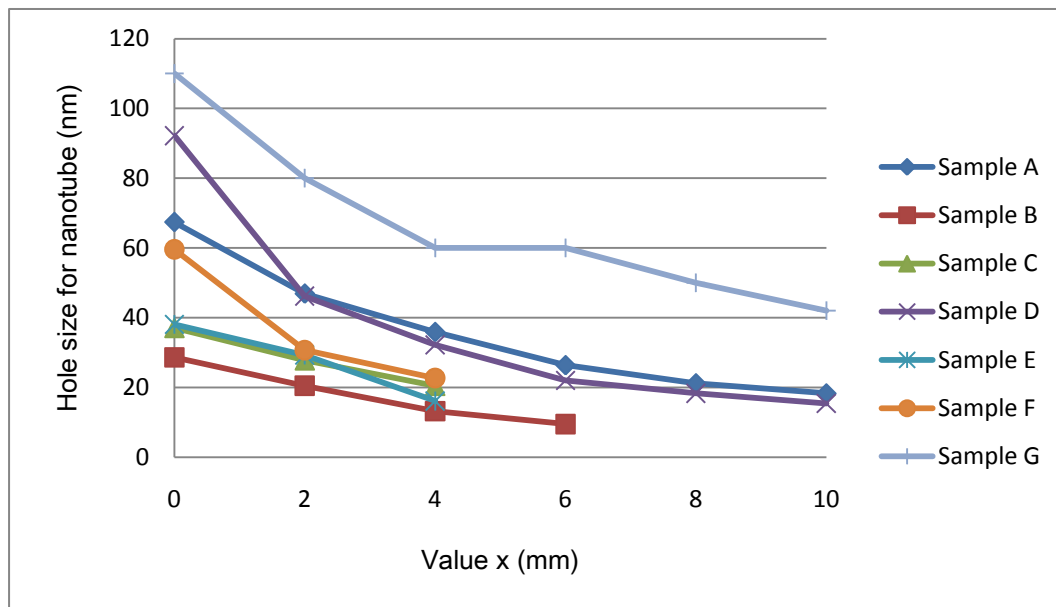


Fig.4.1d The distribution for the hole size of the TiO₂ nanotubes on the sample plane.

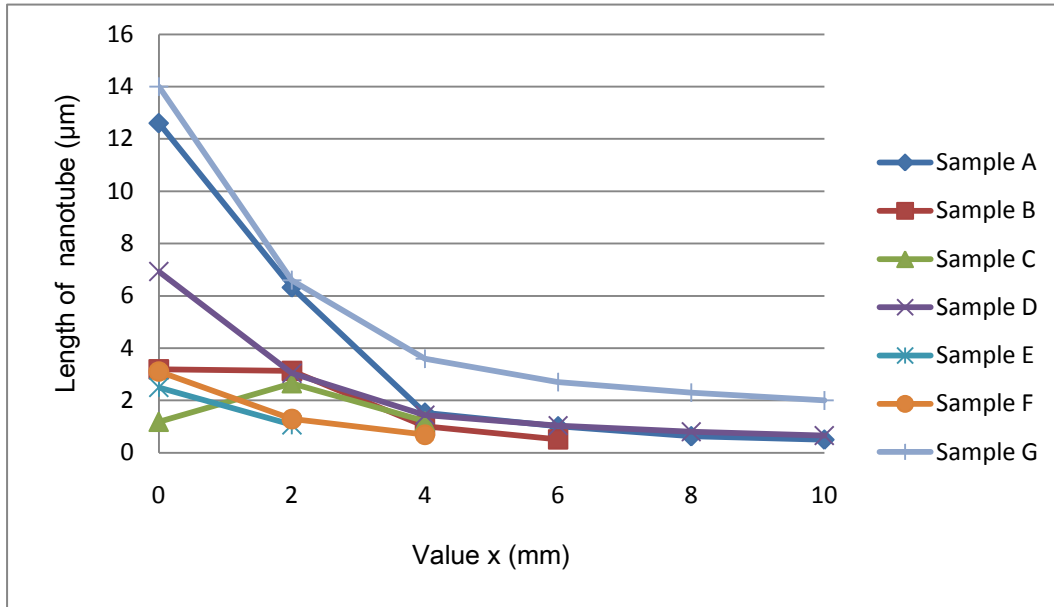


Fig.4.1e The distribution for the length of the TiO₂ nanotubes on the sample plane.

4.2 Comparing the nanostructure of rolled samples and without rolled samples

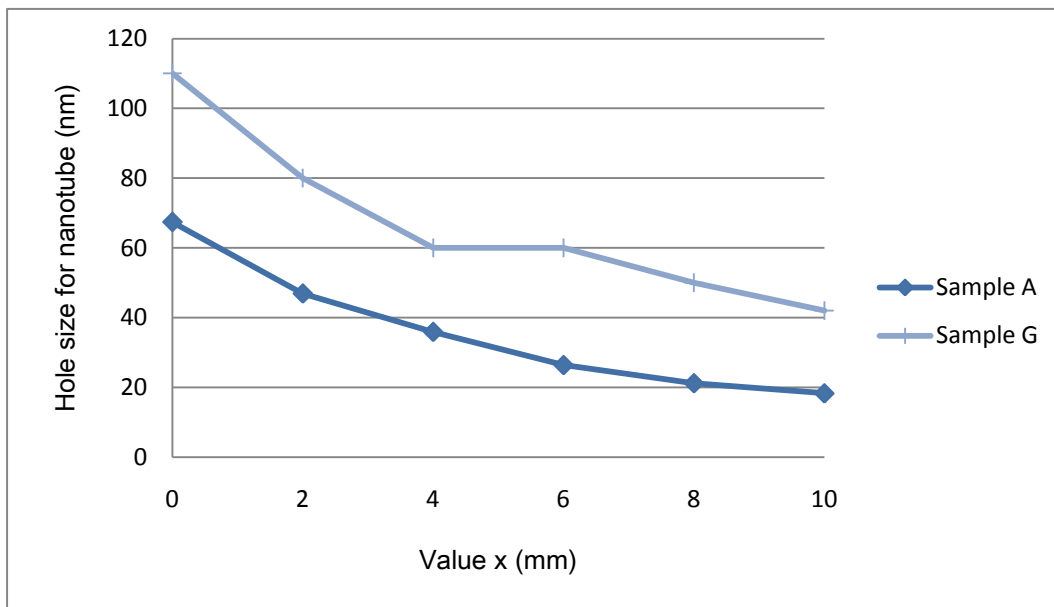


Fig.4.2a Hole size distribution of samples A, G.

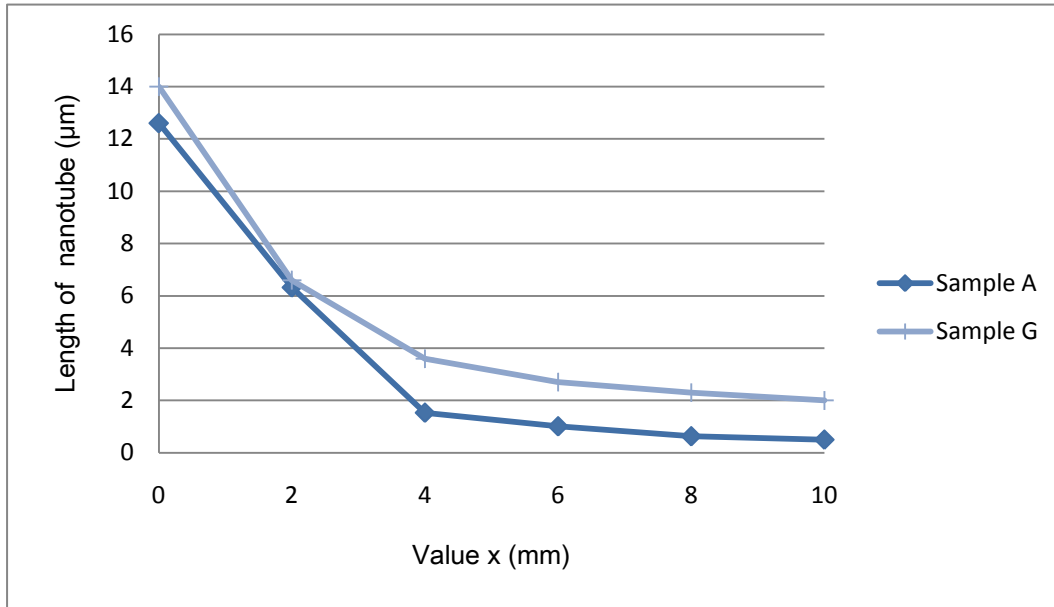


Fig.4.2b Nanotube length distribution of samples A, G.

The effect of cold rolled sample for nanostructure will be discussed here. The hole size of nanotube for sample G was gradually changed from 110 to 42 nm for $x = 0$ to 10mm. For the same anodization condition, the hole size of sample A nanotube change from 67.4nm to 18.3nm for $x = 0$ to 10mm.

When comparing the hole size of the rolled sample and that of without rolled sample, the hole size of sample A is much smaller than sample G. Not only the hole size, but also the length of nanotube is decreases due to the cold rolling. Within the same position, the tube length of sample G and sample A is changes from $14\mu\text{m}$ to $2\mu\text{m}$ and $12.6\mu\text{m}$ to $0.5\mu\text{m}$ respectively.

The hole size and length of nanotube can be decreased by the cold rolling before anodization.

4.3 Comparing the nanostructure between the different values of % cold work

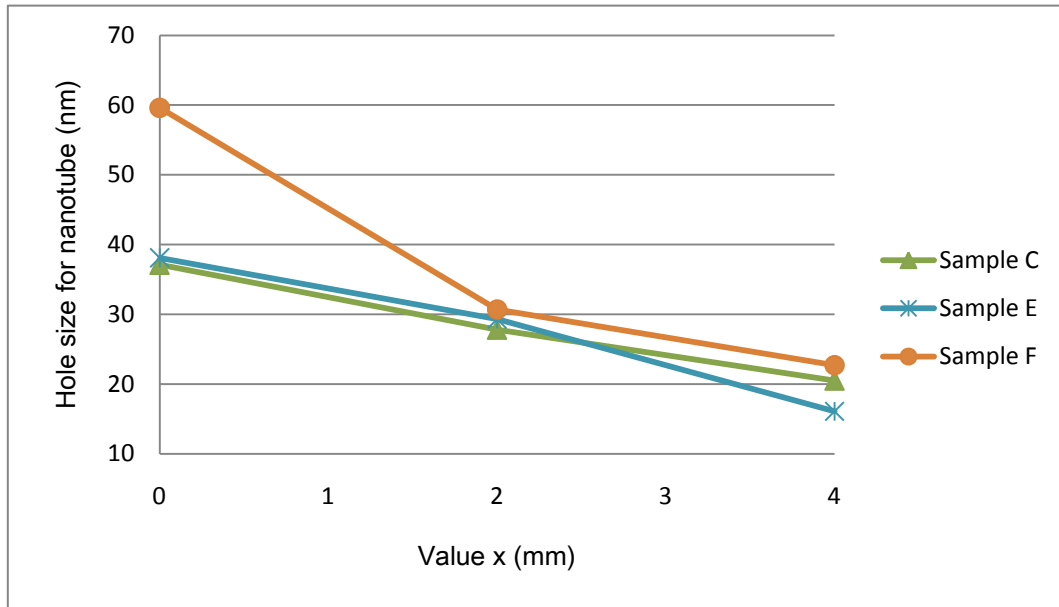


Fig.4.3a Hole size distribution of samples C, E, F.

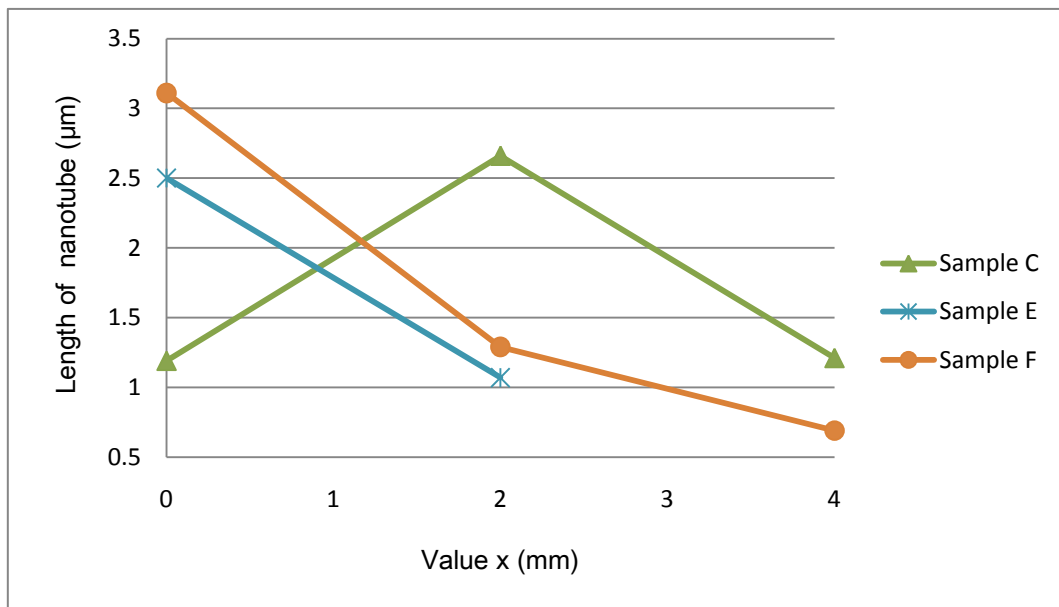


Fig.4.3b Nanotube length distribution of samples C, E, F.

Here the sample for different % cold work with the same anodization condition will be discussed. The % cold work for samples C, E and F, are 60%, 52% and 32% respectively. Fig.4.3a shows that the hole size of sample F is larger than sample E

between $x = 0$ to 4mm and the hole size of sample E is generally larger than sample C between $x = 0$ to 2mm. Fig.4.3b shows that the nanotube length of sample F is longer than sample E between $x = 0$ to 2 and the nanotube length of sample E is generally longer than sample C at $x = 0$.

In the three samples, when the % cold work is high, the hole size and nanotube length will be small and short. Conversely, when the % cold work is low, the hole size and nanotube length will be big and long.

Normally the sample of higher % cold work should have a smaller hole size and shorter nanotube length. It is because a higher % cold work will cause a higher increase in strength. However at $x = 2$ to $x = 4$ mm, sample C appears to produce opposite results. It is because an error appear on sample C between $x = 2$ to $x = 4$ mm.

4.4 Comparing the nanostructure between the different times for anodization

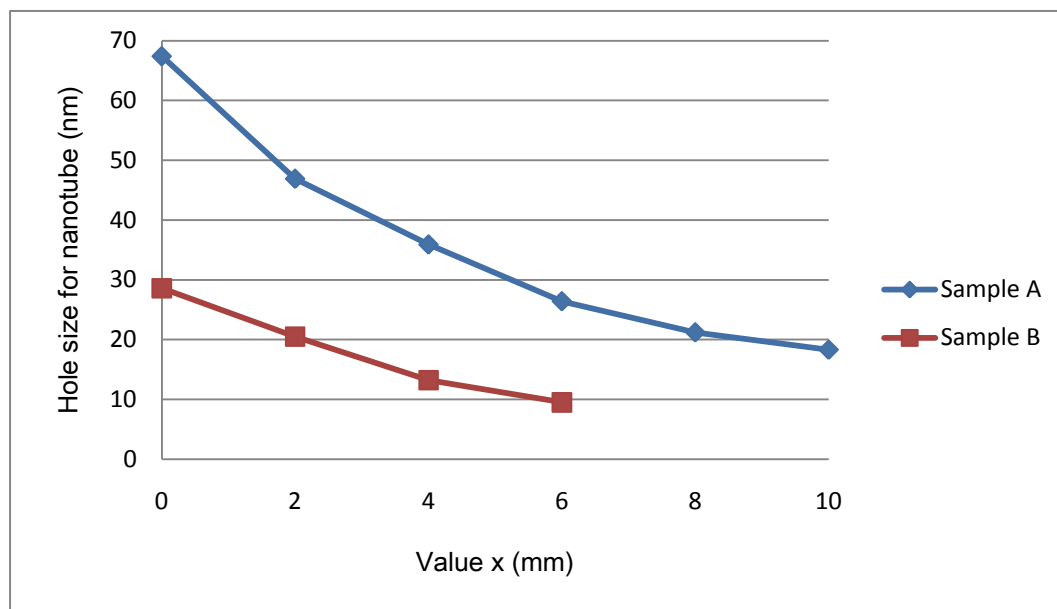


Fig.4.4a Hole size distribution of samples A, B.

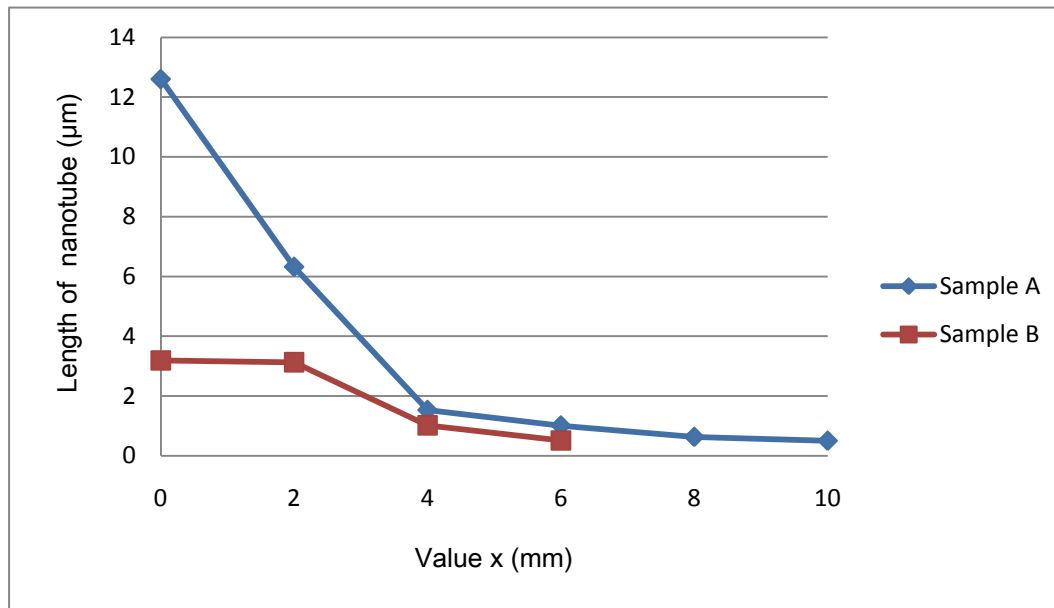


Fig.4.4b Nanotube length distribution of samples A, B.

Through the same % cold work and anodization voltage, the effect of different anodization time for rolled sample will be discussed. The anodization time for sample A and B are 20min and 10min respectively. According to Fig.4.4a, the hole size of sample A and sample B is gradually decreased from 67.4nm to 26.4nm and 28.6nm to 9.5nm between $x = 0$ to $x = 6$ mm. According to Fig.4.4b, the nanotube length of sample A drops rapidly from 12.6µm to 1.01µm between $x = 0$ to $x = 4$ mm and decreased slowly from 1.01µm to 0.5µm between $x = 4$ to $x = 10$ mm. The nanotube length of sample B gradually decreases from 3.19µm to 0.51µm between $x = 0$ to $x = 6$ mm. No nanotube was discovered in sample B after $x = 6$ mm.

The hole size and nanotube length of sample A is larger and longer than sample B at corresponding value x . A longer anodization time will produce a larger hole size and longer length of nanotube. It is because when the anodization time increases, more time is provided for the reaction in anodization, and the effect of anodizing will also increase.

Nanotube was not found in sample B after $x = 6\text{mm}$ for the same reason. When $x = 6\text{mm}$, it means the point of surface that leaves the Pt cathode 6mm . The distance is too far from the cathode and anodization time is not enough. Therefore the effect of anodization is too weak and nanotube cannot be produced in sample B after $x = 6\text{mm}$. Although $x = 10\text{mm}$, nanotubes can be found in sample A. It is because anodization time for sample A is 20min and it is enough to produce nanotubes.

4.5 Comparing the nanostructure between the different voltages for anodization

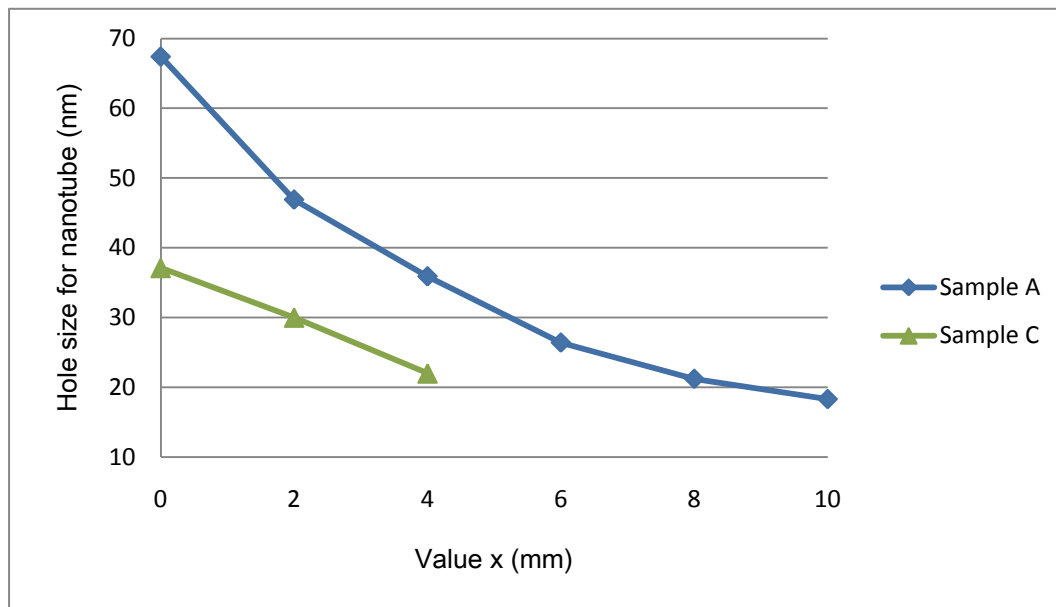


Fig.4.5a Hole size distribution of samples A, C.

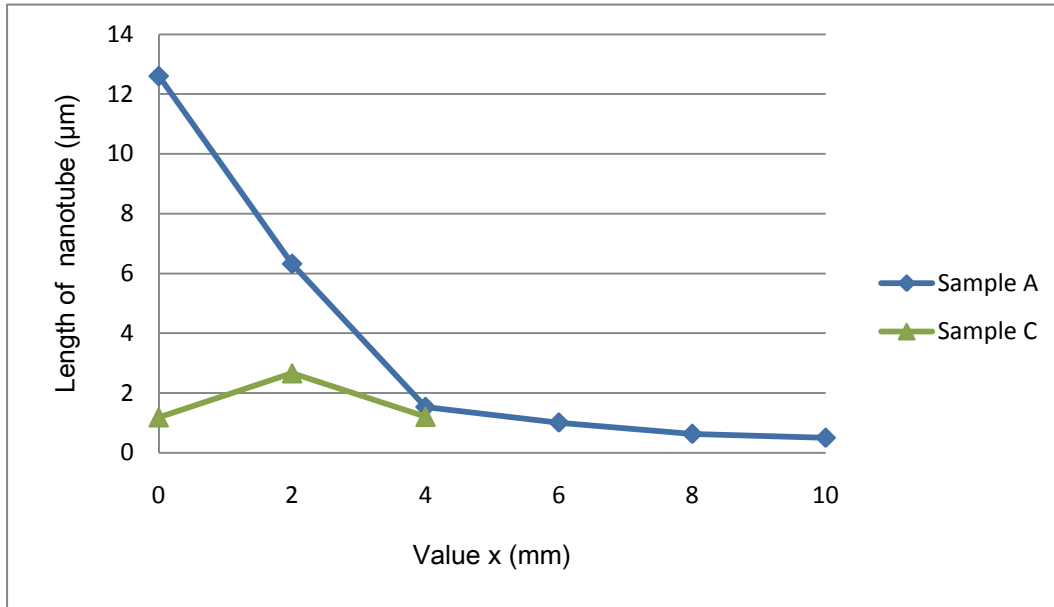


Fig.4.5b Nanotube length distribution of samples A, C.

The effect of nanotube from different anodization voltage with the same % cold work and anodization time will be discussed. The anodization voltage for sample A and C are 100V and 60V respectively. From the Fig.4.5a, the hole size of sample A is gradually decreased from 67.4nm to 18.3nm between $x = 0$ to 10mm. The hole size of sample C is decreased from 37.1nm to 20.5nm between $x = 0$ to 4. According to the Fig.4.5b, the nanotube length of sample A is larger than sample C between $x = 0$ to 4mm. Nanotube was not discovered at sample C after $x = 4$ mm.

A larger anodization voltage will produce a larger hole size and longer length of nanotube. It is because when the anodization voltage increases, the effect of anodizing will also increase.

Nanotube was not found in sample C after $x = 4$ mm because of the low voltage. When $x = 4$ mm, the distance is too far from the cathode and anodization voltage is not enough. Therefore the effect of anodization is too weak and nanotube was not produced in sample C after $x = 4$ mm.

4.6 Reason for the rolling effects of the nanostructure

The properties of metal are dependent on the lattice structure. Cold rolling is a method of work hardening that can affect the lattice structure of metal [25]. After the cold rolling, the dislocation on intersecting slip planes will interact and obstruct each other. This dislocation will accumulate in the material and dislocation density, yield strength and tensile strength will increase [25-28].

Dislocation in the metal may obstruct the anodization process. After the cold rolling, the dislocation density increase and the obstruction also are increase. The size and length of nanotube are decreased by cold rolling.

4.7 Different morphologies of the nanostructure

The changing of the nanotubes morphologies are observed in sample A, D and F. For these sample, porous oxide are appeared at surface for $x = 0$. The tubular oxide are appeared at the surface after $x = 2\text{mm}$. The morphologies at specific condition will change during anodization.

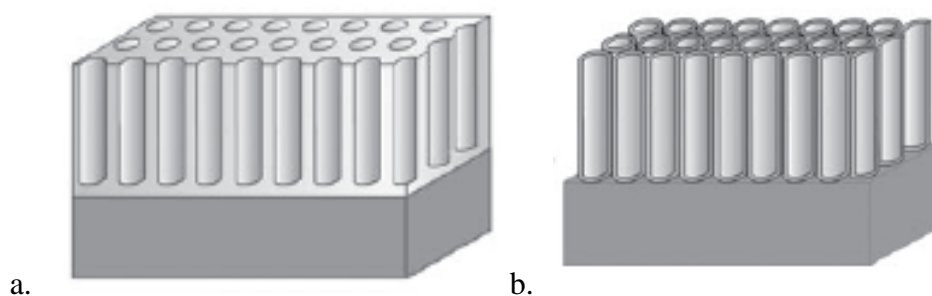


Fig.4.7a Different morphologies (a. porous, b. tubular) are obtained by electrochemical anodization of metallic titanium [23].

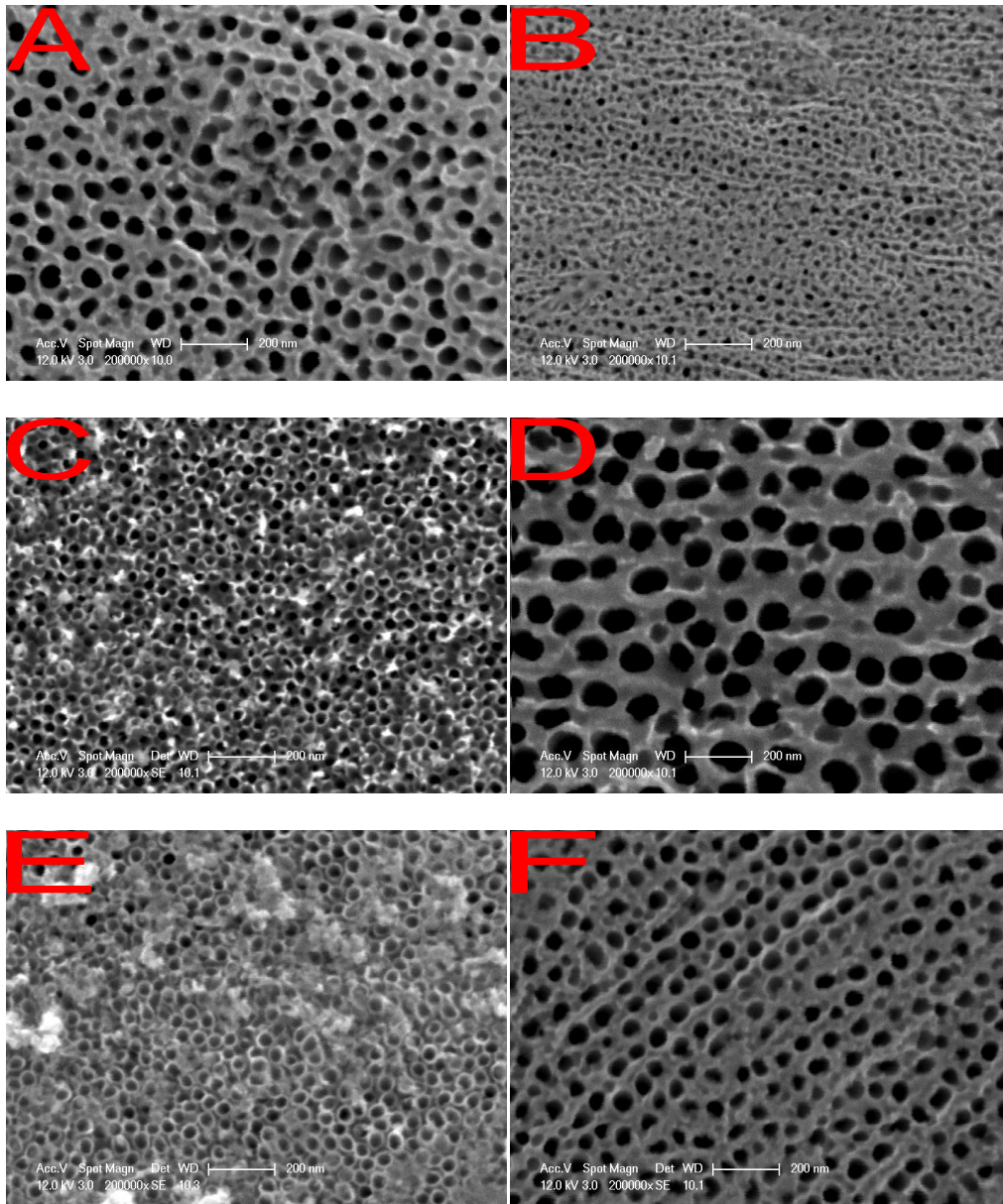


Fig. 4.7b Top-view SEM images of a gradient TiO₂ film of Sample A to F at $x = 0$ (no. A-F respectively).

For the asymmetric electrode configuration of anodization, the IR is dropped follow the gradient direction due to the resistance of the solution. In this condition, the voltage is the highest at $x = 0$. When x is increase, the voltage would decrease at that point of surface. Therefore the morphologies are changed due to the voltage during anodization. When the voltage is high, porous structure is obtained. When the voltage is low, tubular structure is obtained.

When comparing sample A to F, only A, D and F appears porous structure. Tubular structure is appeared at other sample. The main different between them is the anodization voltage. Sample A, Band D are fabricated through 100V anodization. Other samples are fabricated through 60V anodization. Therefore sample A and D appears porous structure at $x = 0$ is due to the high voltage.

Sample B is fabricated through 100V anodization but porous structure haven't appear. It is because the anodization time is too short. On the other hand, although sample F is fabricated through 60V anodization but appear the porous structure at $x = 0$. It is because the % cold work is too low.

5 Conclusion

The dimension and length of gradient TiO₂ nanotube arrays are successfully changed by cold rolling before anodization. Rolled Ti foils are used to fabricate a gradient TiO₂ nanotube arrays through anodization using an asymmetric electrode configuration. The changing of tube diameters and length are dependent on the % cold work. When the % cold work is high, the dimension and length of nanotubes will be small and short. Conversely, when the % cold work is low, the dimension and length of nanotubes will be big and long.

The effect of anodization time and voltage for rolled Ti foils are studied. A longer anodization time and larger voltage will produce a larger dimension and longer length of nanotubes. It is because when the anodization time or voltage increases, the effect of anodizing will also increase.

After the cold rolling, the dislocation density increases and the obstruction of anodization also increases. Therefore the size and length of nanotubes are decreased by cold rolling. Different nanotube morphologies are studied. The morphologies are changed due to the voltage during anodization. When the voltage is high, porous structure is obtained. When the voltage is low, tubular structure is obtained.

Reference

- [1] Boyce E. Collins, Keiki-Pua S. Dancil, Gaurav Abbi, and Michael J. Sailor, Determining Protein Size Using an Electrochemically Machined Pore Gradient in Silicon, *Adv. Funct. Mater.* 2002, 12, No. 3, March.
- [2] Yang Yang Li, Peter Kim, and Michael J. Sailor, University of California, Department of Chemistry and Biochemistry, San Diego, CA, USA Painting a rainbow on silicon – a simple method to generate a porous silicon band filter gradient, 2005.
- [3] Amiya Kumar Patel, Use of Electrochemically Machined Porous Silicon to Trap Protein Molecule, 10 May 2010.
- [4] D. Navarro-Urrios, C. Pérez-Padrón, E. Lorenzo, N. E. Capu, Z. Gaburro, C. J. Oton and L. Pavesi, Chemical etching effects in porous silicon layers, 29 April 2003.
- [5] Jian-Wen Cheng, Chun Kwan Tsang, Fengxia Liang, Hua Cheng and Yang Yang Li, Department of Physics and Materials Science, City University of Hong Kong, Kowloon, Hong Kong, P.R. China, Gradient TiO₂ nanotube array, 2010.
- [6] Craig A. Grimes, *J. Mater. Chem.*, Synthesis and application of highly ordered arrays of TiO₂ nanotubes, 2007, 17, 1451–1457.
- [7] Evgeny Katz, Department of Chemistry & Biomolecular Science, Clarkson University, Reference Electrode Page, 2007.
<http://people.clarkson.edu/~ekatz/refelectrodes.htm>.

- [8] Robert S. Alwitt, Boundary Technologies, Inc., Electrochemistry Encyclopedia, December, 2002.
<http://electrochem.cwru.edu/encycl/art-a02-anodizing.htm#dtop>
- [9] From Wikipedia, the free encyclopedia, Anodizing.
http://en.wikipedia.org/wiki/Anodizing#Anodized_titanium
- [10] Mario S Pennisi and Derek Jones, ANODISING.
<http://www.coatfab.com/anodising.htm>
- [11] Anodising. <http://www.valhallaarms.com/wyvern/titanium/anodizing.htm>
- [12] From Wikipedia, the free encyclopedia, Scanning electron microscope.
http://en.wikipedia.org/wiki/Scanning_electron_microscope
- [13] Lecture notes of AP3171 Materials Characterization Techniques, City University of Hong Kong –Scanning Electron Microscopy.
- [14] Lecture notes of AP4178 Nanostructures & Nanotechnology, City University of Hong Kong –Characterization, p3-8, 39.
- [15] From Wikipedia, the free encyclopedia, Field emission gun
http://en.wikipedia.org/wiki/Field_emission_gun
- [16] PhotoMetrics, Inc., Field Emission Scanning Electron Microscopy (FESEM)
<http://www.photometrics.net/index.html>
- [17] From Wikipedia, the free encyclopedia, Work_hardening
http://en.wikipedia.org/wiki/Work_hardening
- [18] Serdar Z. Elgun, Cold Work.
<http://info.lu.farmingdale.edu/depts/met/met205/coldwork.html>

- [19] Lecture notes of AP3110 Deformation and Fracture, City University of Hong Kong –Strengthening mechanism.
- [20] Lecture notes of AP4178 Nanostructures & Nanotechnology, City University of Hong Kong –Synthesis of onedimensional(1D) nanomaterials.
- [21] <http://web.pdx.edu/~pmoeck/phy381/coldworking.pdf>
- [22] Craig A. Grimes & Gopal K. Mor, TiO₂ Nanotube Arrays Synthesis, Properties, and Applications, Pennsylvania State University Electrical Engineering Department, 2009.
- [23] Andrei Ghicov and Patrik Schmuki, Self-ordering electrochemistry: a review on growth and functionality of TiO₂ nanotubes and other self-aligned MO_x structures, 6th April 2009
- [24] Serdar Z. Elgun, MATERIAL SCIENCE - Laboratory: Cold Working
<http://info.lu.farmingdale.edu/depts/met/met205/index.html>
- [25] I. Schindler, M. Janošec, E. Místecký, M. Růžička, L. Èřek, L.A. Dobrzański, S. Rusz, P. Suchánek, Archives of Materials Science and Engineering, Effect of cold rolling and annealing on mechanical properties of HSLA steel, Volume 36 Issue 1 March 2009 Pages 41-47.
- [26] Hanliang Zhua, A.K. Ghoshb, K. Maruyamaa, a Graduate School of Environmental Studies, Tohoku University, USA Received in revised form 28 November 2005; accepted 2 December 2005
- [27] Mikell P. Groover, ISE 311 Rolling lab, Chapters 18 and 19 in the text book “Fundamentals of Modern Manufacturing”, Third Edition, May 22nd, 2008.

- [28] From Wikipedia, the free encyclopedia, Rolling (metalworking).
http://en.wikipedia.org/wiki/Rolling_%28metalworking%29
- [29] From Wikipedia, the free encyclopedia, Titanium dioxide.
http://en.wikipedia.org/wiki/Titanium_dioxide
- [30] Anodizing Titanium. http://www.bme.unc.edu/~bob/bob_titanium.html
- [31] Yanbo Li, Maojun Zheng, Li Ma and Wenzhong Shen, Laboratory of Condensed Matter Spectroscopy and Opto-Electronic Physics, Department of Physics, Shanghai Jiao Tong University, Shanghai 200240, People's Republic of China, Fabrication of highly ordered nanoporous alumina films by stable high-field anodization, Online at stacks.iop.org/Nano/17/5101
- [32] Xiaoliang Yuan, Maojun Zheng, Li Ma and Wenzhong Shen, Key Laboratory of Artificial Structures and Quantum Control, Ministry of Education, Department of Physics, Shanghai Jiao Tong University, High-speed growth of TiO₂ nanotube arrays with gradient pore diameter and ultrathin tube wall under high-field anodization, Online at stacks.iop.org/Nano/21/405302.